Three Dimensional Diffraction Imaging

Leigh Martin

Research Group of Dr. John Miao, Physics and Astronomy Department, UCLA

1 Introduction

Microscopy has incited many of the greatest revolutions in scientific history. In particular, these inventions have sparked paradigm shifts in biology, and discoveries like the structure of DNA are indebted to such studies. The development of the field spans from recent work like scanning electron microscopy and atomic force microscopy to the original optical microscope, which dates back hundreds of years.

However, despite the legacy of the field, many structures remain difficult to probe with current methods. For example, many complex, non-crystalline structures remain largely unexplored at the nanoscale. These limitations stem from the fundamental properties of the imaging particles used. The diffraction limit prevents optical microscopes from imaging details significantly finer than the wavelength of light used. Electron microscopes have much shorter wavelengths at their disposal, but the small penetration depth can prevent full structure determination. While x-ray crystallography allows full, atomic resolution images of samples, it requires vast arrays of identically oriented samples, which is often not feasible for amorphous structures like glass and complex biological matter.

Diffraction Imaging has, in recent years, promised to circumvent many of these limitations. Novel algorithms for solving the phase problem and high-flux coherent light sources are enabling imaging with a wide range of electromagnetic wavelengths. In addition, the technique does not rely on lenses, which avoids problems associated with focusing short-wavelength light. A coherent light source and suitable detector suffice to produce quality images.

The focus of this article is on developments in a recent addition to diffraction imaging called Ankylography. Ankylography generalizes diffraction imaging to three dimensions in certain cases. Before going into the details of this technique, a review the two dimensional case is appropriate.

2 Coherent Diffraction Imaging

In conventional coherent diffraction imaging (CDI), light scattered from a finite sample is directly measured at a detector placed in the Fraunhofer region. In this region, where the

diffraction angle θ is small enough that it satisfies the relation $sin\theta \cong \theta$, the intensities measured at the detector satisfy:

$$I(x', y') \propto |F[g(x, y, z)](x', y', 0)|^2 \qquad (1)$$

Where g(x,y,z) represents the scattering amplitudes of the object, x' and y' are the detector coordinates and F is a Fourier transform. z' = 0 signifies that no information along the beam direction axis is contained in the diffraction pattern except for the zero order term, which is equivalent to an integral along the z (a projection). This is the basic result of Fourier optics[1]. Finally, conventional CDI requires that the object be bounded, and that outside this bounding region, the object's amplitudes must be zero.

The Fourier transformation is invertible, so one might expect the above relation to easily yield information about the object. However, the phase is not measured directly, so the Fourier transform cannot be immediately inverted. Fortunately, it has been found that the phase may be recovered by oversampling the diffraction pattern.

Oversampling, simply put, is measuring the diffraction pattern more finely than is required for inversion of the Fourier transform (sampling higher than the Nyquist frequency)[2]. If an object is of finite extent, than the spatial frequencies in its diffraction pattern are limited. Without going into the mathematical details of Nyquist-Shannon Sampling Theorem, this can be made intuitive by thinking of the object as the Fourier transform of the diffraction pattern (which is correct up to a phase factor). The diffraction pattern is band-limited because the object is zero outside some finite region (this finite region is called the support). Therefore, there is a maximum level of detail contained in the diffraction pattern, and sampling more finely than the highest band yields redundant information (as illustrated in figure 1). Diffraction imaging utilizes this redundant information, and the extra constraints allow determination of the unmeasured phase[3].

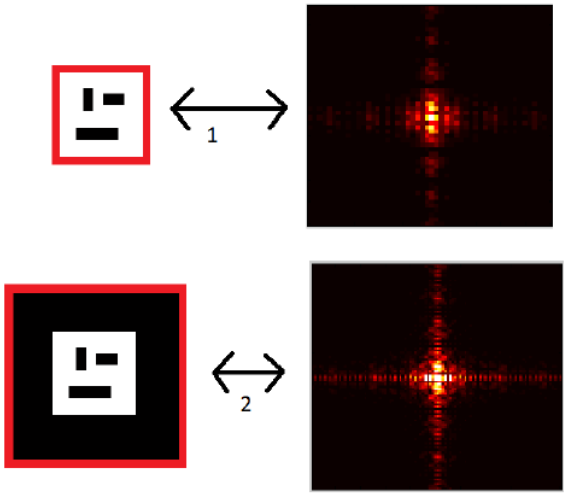

Figure 1: The left images are R-space and the right images are their Fourier transforms. The second diffraction pattern is sampled at twice the level of detail, but the IFFT of the diffraction pattern only contains a zero-padding region; no new information about the object is present

CDI reconstructs the phase by use of an iterative algorithm. The first efficient algorithm developed was the Hybrid Input Output (HIO) algorithm[3]. In this method, a random phase guess is chosen for each point on the diffraction pattern. Then, an inverse Fourier transform obtains the first estimate of the object. In general, this real-space image does not have a finite support (i.e. it does not have a finite region outside which its amplitudes are zero). As CDI requires that the object be have this property, the algorithm enforces the constraint by pushing the amplitudes to zero using the following relation:

$$g_{k+1} \rightarrow \begin{cases} g_k \\ g_k - \beta g_k' \end{cases}$$

Where $g_{k'}$ is the object estimate with the Fourier modulus constraint enforced and g_k is the object domain without this constraint enforced[3]. This particular combination of g and g' is a subset of a general class of what are called difference maps. These difference maps generalize the HIO, and the underlying theory explains why the HIO is so much more efficient than previously developed algorithms (such as the Gerchberg-Saxton Algorithm). This theory is outside the scope of this article, but an excellent treatment is given in reference 4.

3 Ankylography

Since its first demonstration in 1999[5], two dimensional CDI has been demonstrated numerous times, both computationally and experimentally[2,3,5,6,7,8]. In 2010, Raines et. al. published a novel method called Ankylography, which generalizes CDI to three dimensions. This modality requires collection of large diffraction angles, so that the small angle approximation no longer holds, and the wave front is no longer planar, but spherical. In this context, the z term in the Fourier transform is no longer zero as in equation (1), but varies with the diffraction angle θ like cosθ-1. This unique geometry is represented in figure 2[1], and can be derived using the Born approximation[9]. The hemisphere is called the Ewald sphere. Two are present because of centrosymmetry of the K-space, which comes from the fact that a the measured object is real.

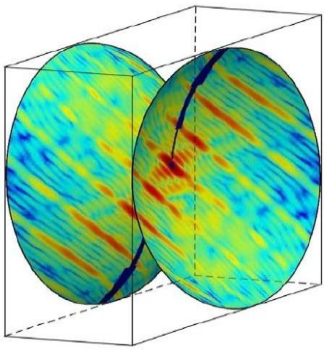

Figure 2: The diffraction pattern embedded in 3 dimensional space. Notice that significant volumes of data are unknown.

As shown in this figure, only a 2 dimensional slice of the object's K-space is measured. Ankylography uses the HIO not only to reconstruct the phases in the measured diffraction, but also to reconstruct phases and amplitudes in the undetermined volumes. Once these values are determined, full 3 dimensional scattering amplitudes of the object are revealed. The method

[1]Image Source: CC Chen et. al., Three-Dimensional Imaging of a Phase Object from a Single Sample Orientation by Using an Optical Laser, pre-publication

has been demonstrated in both simulation and experiment, but the full capabilities remain largely unexplored. Also, the importance of various parameters such as oversampling degree, and the various techniques used to improve reconstructions can be quantitatively explored in more detail.

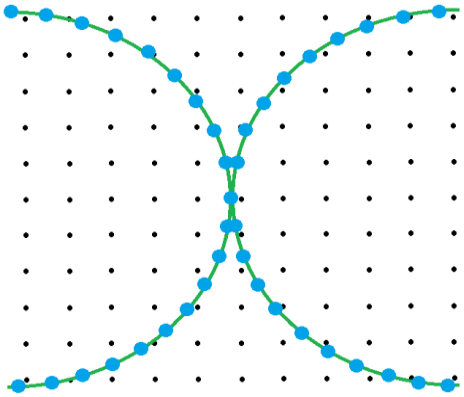

Figure 3: Measured points (blue) embedded in the Cartesian K-space (black points)

Experimental details of Ankylography are also significant to the robustness of the technique. Perhaps the most important is the interpolation process. In real experiments, and even simulations, all data are discreet in nature. The diffraction pattern is measured using a finite number of pixels on a flat detector (which easily maps to a uniformly curved sphere by projecting onto the Ewald sphere and normalizing[10]). Similarly, the object and its K-space are represented as finite arrays inside the computer. In order to represent the Ewald sphere in this array, one must interpolate from the measured points on the detector to the nearest points in the K-space voxel array. Figure 3 shows a graphical representation of this detail. Note that the spacing of the points in the Cartesian grid relates to the oversampling degree. Many interpolation methods, including linear, bi-linear and spline interpolation methods prove useful in matching measured data as closely as possible with reconstruction data.

Ankylography has been proposed not only as a method of obtaining 3 dimensional information from one view, but also as a way to reduce the number of projections required for tomography given multiple views. In this context, multiple Ewald spheres reside in the same K-space and further constrain details of the object. As Fourier transformations and rotations commute, the Ewald spheres are placed in the Fourier domain rotated at the same angle and along the same axis as the object. See figure 4 for an image of this construction.

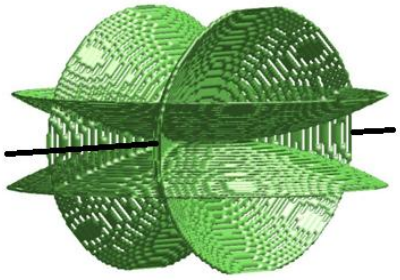

Figure 4: Two projections from an object rotated 90° about an axis parallel to the black line. The low curvature compared to a full hemisphere corresponds to a maximum diffraction angle less than 90°.

4 Simulations and Results

As having a greater number of known values than unknown values imposes more constraints on the object, it was expected that the oversampling degree and the number of projections would improve reconstructions. To verify these expectations, simulation were run which reconstructed an object under a variety of conditions. A confocal image of a neuron was

used as a test sample[2], which consisted of a 32*32*8 voxel array. This array was embedded in a cubic array of a size that determined the oversampling degree. Ankylography was simulated by taking the Fourier transform and then eliminating information about points outside of the Ewald spheres. The curvature of the Ewald spheres was chosen such that the diffraction angle was 39 degrees. The 3 dimensional HIO was run with a rectangular support around the object. Note that this is an idealized case, because it ignores issues of interpolation.

As samples are often mounted on membranes rather than suspended in free space, the choice of projection angles should reflect this geometry. When the beam is normal to the membrane, no diffracted light is blocked by the membrane or the material on which it is mounted. However, at 90° to this, the beam would collide with the membrane and diffracted light would be blocked. As the diffraction angle is 39°, the rotation angles were chosen so as to not block any diffracted light. In the end, angles were limited between -45° and +45°, and were equally spaced within this range for each run.

Reconstructions started by choosing the best of 40 random seeds. Each seed is the result of 70 iterations of the 3D HIO, and the starting phase guess is recorded. The best seed was selected based on how well points on the spheres corresponded with points on the known Ewald spheres. This 'K-space error' is also important for measuring the quality of the final reconstruction. At a given iteration, it is calculated by taking the current object estimate and setting all points outside the support to zero. The Fourier transform of this is compared to the known amplitudes on the Ewald sphere[3].

Performing reconstructions with multiple parameters requires many reconstructions, (and 40 times as many seeds, in this case), so the number of reconstructions required quickly becomes unfeasible to run one-by-one. Therefore, bash script was written to automate the seeding process. The code first calls matlab to generate a random seed and create a Fourier domain array for reconstruction. It then runs a multi-threaded HIO code (which parallelizes the Fast Fourier transform) to reconstruct the object. After saving the error and the random seed and repeating many times, the code finds the best seed and carries out the reconstruction for additional 2000 iterations.

Figure 5 shows a series of 225 reconstructions using a set of 25 combinations of parameters. Each of the 25 was run 9 times in order to verify the results and quantify the error. The vertical axis is the percent K-space error described above. As expected, a greater number of

[2] Special thanks to Christopher J. Tabone, who has granted permission for use of these data.

[3] This method closely mimics a method used to quantify error in 2 dimensional CDI, in which the K-space error is quantified by running several iterations of the Gerchberg-Saxton algorithm. This algorithm is observed to quickly reduce the magnitudes outside the support. After these iterations, the known and measured Fourier transforms are compared.

projections yields a lower error, and hence a better reconstruction. However, the oversampling ration seems to be unhelpful, if not detrimental to reconstructions. It is known that phase and amplitude retrieval are not possible if the oversampling ratio is too small, but it appears that this trend does not extrapolate to very large oversampling degrees.

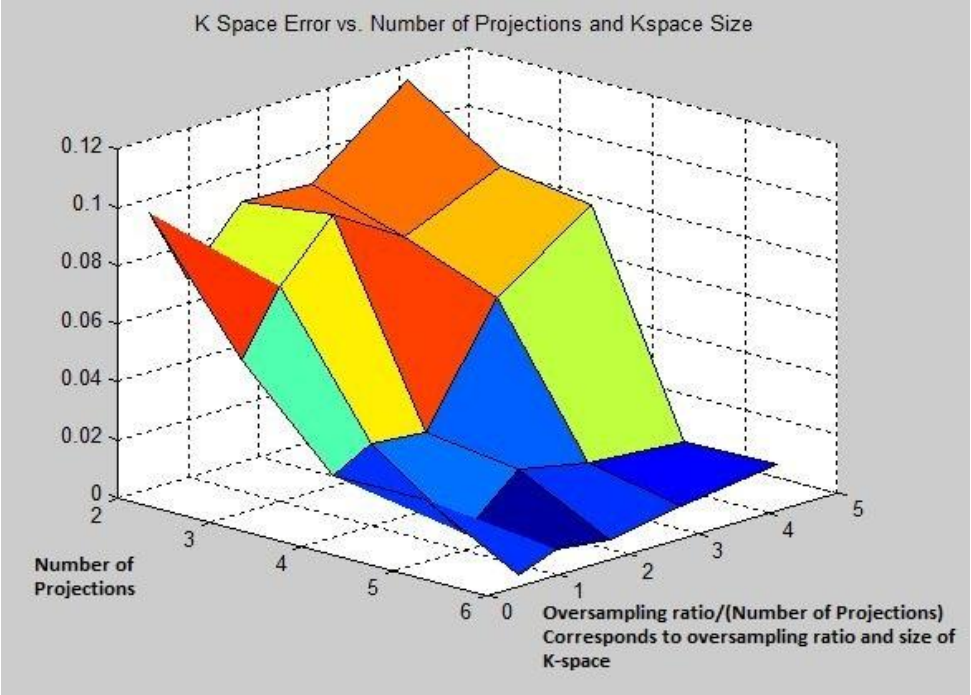

Figure 5: 25 combinations of oversampling degree and number of projections. They form a 5x5 grid of error values. Each value is determined from 9 independent, seeded reconstructions. Error bars are +/-.01 on average, based on the standard deviation. Oversampling ration is defined to be the number of points inside the support divided by the number of known points.

A larger oversampling ratio means the voxel array is larger, so it was possible that the larger reconstructions had simply not converged as far as the smaller ones. However, this possibility was not supported by looking at the rate of change of the error at the end of the reconstruction. Figure 6 shows a plot of the derivative of the error as a function of the number of projections and the normalized oversampling ratio. There is no apparent trend in the convergence, which supports the statement that the oversampling ratio is not benefitting these reconstructions.

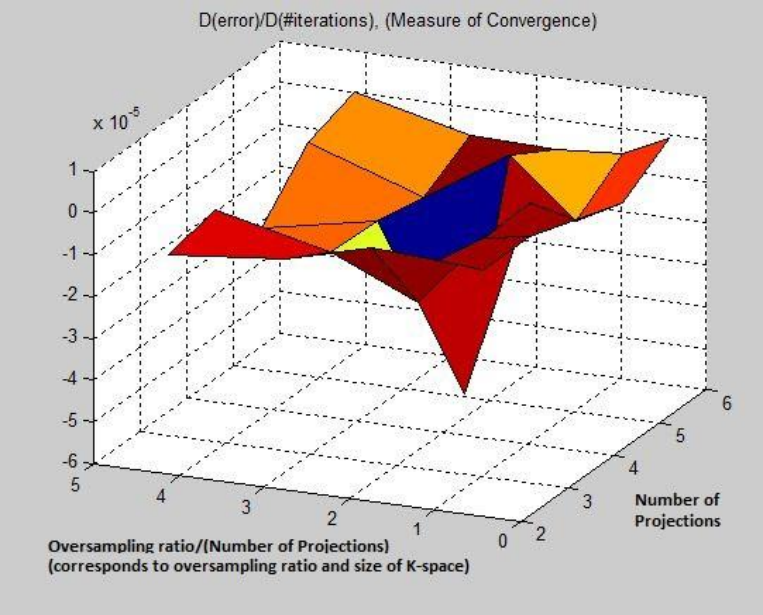

Figure 6: Reconstructions error is still decreasing slightly, but the rate of change is not correlated with either parameter.

These results were repeated with a small missing center in the diffraction pattern. In figure 7, the same parameters were used, except that a 4° region in the zero order of the diffraction pattern was removed. Figure 7 shows the results of these simulations. The salient features are consistent with the results from figure 5

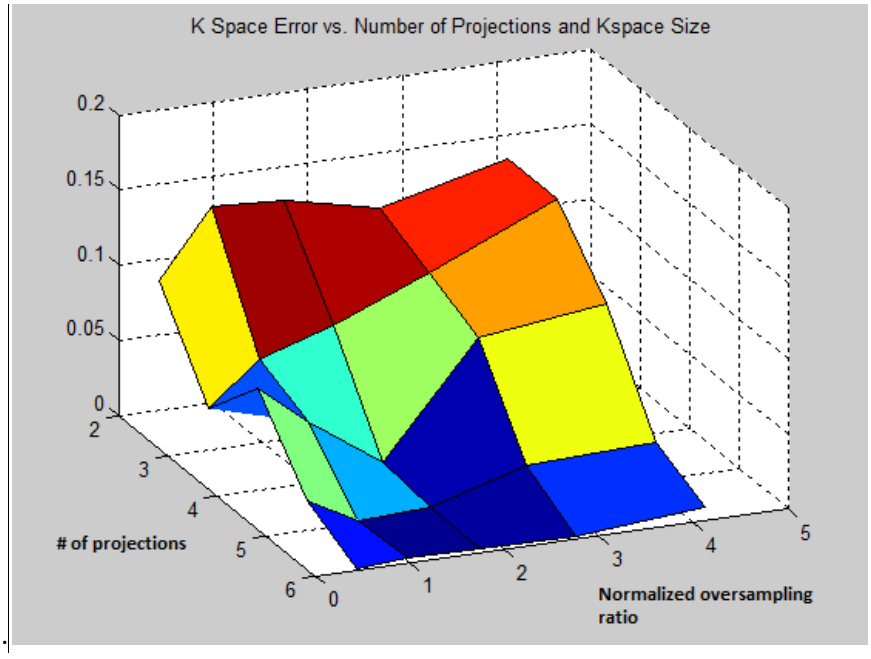

Figure 7: 225 independent reconstructions plotted in the same manner as figure 5. The only difference is the presence of a small missing center in the diffraction pattern.

5 Conclusions

These results are for a relatively thin sample, which was chosen because it corresponds to a biological sample which we have proposed to measure. The sample is a neuron mounted on a thin membrane, and the proposed illumination wavelength is 543nm. In multiple-projection Ankylography, the x, y and z resolution should all be the same. Given a collection angle of 39°, the resolution is $\frac{\lambda}{\sin(\theta)} = .86\ \mu m$[4], which means there are .43µm per pixel. This means that our 32x32x8 voxel array corresponds to a neuron which is 13x13x3 µm. These dimensions closely match those of the proposed sample. Therefore, the simulations suggest an optimal configuration for the physical CDI experiment. By comparing reconstructions based on K-space error, real-space error and visual appearance, it was found that 4 projections (without a missing center) yield excellent qualitative and quantitative reconstructions. Figure 8 shows one such reconstruction. The R-space RMS error is less that 5%. Shown alongside is a corresponding reconstruction using a small missing center. The R-space RMS error is 10% in this case, but the reconstruction appearance is still quite good.

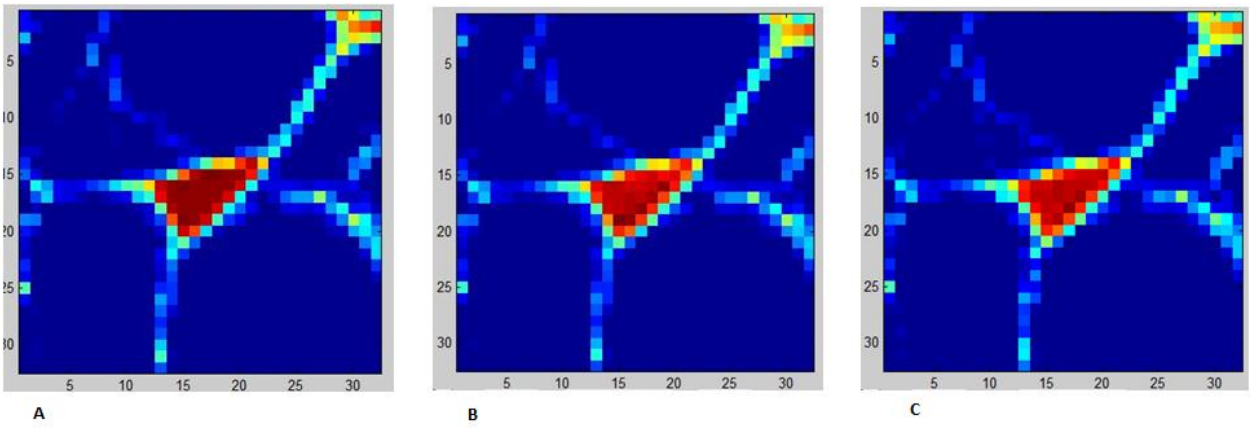

Figure 8: A: A slice of the original sample.
B: Reconstruction using 4 projections and a 128x128x128 K-space array
C: the same reconstruction with a 2 degree missing center (4 degrees side to side)

The fact that the number of projections helped the reconstructions is not surprising, as more data are known in the missing volumes. The question of how the oversampling degree affects the reconstructions was a more open question. Simulations seem to show that a higher oversampling degree does not benefit reconstructions after a point. However, it is known from experiment that oversampling ratio is critical to reconstruction quality. The simulations suggest that this is not due to the fact that the diffraction pattern contains more information, so an alternative explanation is necessary.

[4] Note that this usage of theta differs from another common usage in which 2θ is the diffraction angle.

The following diagram may shed light on this issue. Points on the Ewald sphere do not exactly match up with points on the Cartesian grid. Interpolation seeks to match up pixels on the detector with points on the grid. What is important to notice is that even if interpolation in angular coordinates were perfect, there is still some error due to the fact that points on the Cartesian grid mostly lie slightly off the Ewald sphere. When the oversampling ratio is higher, this discrepancy is made smaller, as is apparent from figure 9. This may account for the simulated and experimental observations regarding the oversampling ratio.

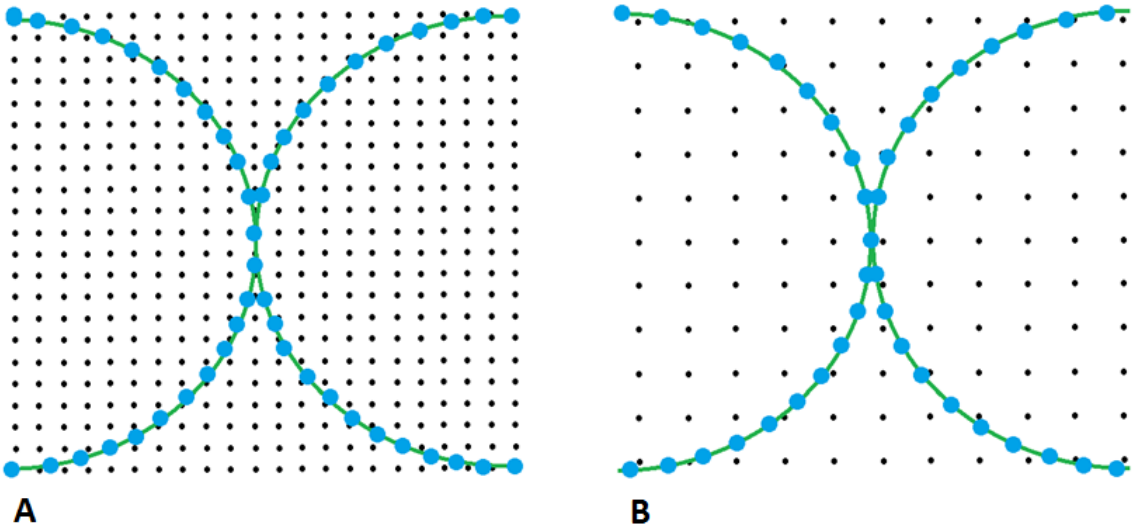

Figure 9: Case A uses a higher oversampling degree than B, and consequently, points on the Ewald sphere are closer to points on the Cartesian grid.

6 Current and Future Directions

These results suggest first and foremost that the interpolation problem is vital to the efficacy of Ankylography. Increasing the oversampling ratio is one possible solution. Another involves incorporating the interpolation process into the reconstruction process. One technique proposed by CC Chen et. al. actively searches for an extension off of the Ewald sphere onto the nearby Cartesian grid points. This algorithm requires operations which appear more computationally intensive than an FFT. However, if the oversampling ratio is less fundamentally significant to reconstructions than previously thought, this problem could be overcome by using smaller K-space arrays and instead interpolating larger distances.

Another proposed direction is to use the shrink-wrap method. This method has been generalized to 3 dimensions and work is being done to determine its applicability to Ankylography. The method actively finds a tighter estimate of the support as the algorithm runs, and has been highly useful in CDI. As a tighter support correlates strongly with better reconstructions, it is expected that this method will improve the reconstructions.

Simulations are currently underway which repeat figures 5 and 7 using a larger, cubic object. This is the first step towards a series of simulations to test how many unknown voxels Ankylography is fundamentally capable of reconstructing, which has been a large area of debate in the field.

Overall, these simulations support Ankylography as a technique and show that it may be useful in many contexts. The proposed bio-imaging project using multiple projections from a neuron sample is important because it could potentially obtain better resolution than confocal microscopy, the current standard in the field. Not only is the technique only constrained by the diffraction limit, but it has the potential for imaging with lower light exposure, which could allow the extension to shorter wavelengths. In addition, it does not require fluorescent tagging, which is currently ubiquitous in the field.

Though only at its inception, Ankylography already shows promise for imaging unexplored materials. With proper theoretical and practical development, Ankylography may one day generate images of biological matter with unmatched detail. The method is quite difficult to implement, so this possibility may only be realized with concentrated efforts to understand the simple cases and generalize these to more elusive objects. Even given the current level of demonstration, Ankylography promises to produce useful and unexplored way.

References

1. Cowley, C., 1995, Diffraction Physics, 3rd. Edition. (North-Holland personal library).
2. J. Miao, et. al., “Phase Retrieval from the Magnitude of the Fourier transform of Non-periodic Objects”, J. Opt. Soc. Am. A. A 15, 1662-1669 (1998)
3. Fienup, J. R. (1978). Reconstruction of an object from the modulus of its Fourier transform. Optics letters, 3(1), 27–29. OSA. Retrieved January 19, 2011, from http://www.opticsinfobase.org/abstract.cfm?URI=ol-3-1-27.
4. Elser, V. (2003). Phase retrieval by iterated projections. JOSA A, 20(1), 40–55. Optical Society of America. Retrieved January 19, 2011, from http://www.opticsinfobase.org/abstract.cfm?URI=JOSAA-20-1-40.
5. J. Miao, P. Charalambous, J. Kirz and D. Sayre, Extending the methodology of X-ray crystallography to allow imaging of micrometre-sized non-crystalline specimens, Nature 400, 342-344 (1999).
6. Thibault, P., & Rankenburg, I. C. (2007). Optical diffraction microscopy in a teaching laboratory. American Journal of Physics, 75(9), 827. doi: 10.1119/1.2750378.f
7. Chapman, H. N., & Nugent, K. A. (2010). Coherent lensless X-ray imaging. Nature Photonics, 4(12), 833–839. Nature Publishing Group. doi: 10.1038/NPHOTON.2010.240.
8. Sandberg, R., Paul, A., Raymondson, D., Hädrich, S., Gaudiosi, D., Holtsnider, J., et al. (2007). Lensless Diffractive Imaging Using Tabletop Coherent High-Harmonic Soft-X-Ray Beams. Physical Review Letters, 99(9), 1-4. doi: 10.1103/PhysRevLett.99.098103.
9. Raines, K. S., Salha, S., Sandberg, R. L., Jiang, H., Rodríguez, J. a, Fahimian, B. P., et al. (2010). Three-dimensional structure determination from a single view. Nature, 463(7278), 214-7. doi: 10.1038/nature08705.
10. Raines, K. S., Salha, S., Sandberg, R. L., Jiang, H., Rodríguez, J. a, Fahimian, B. P., et al. (2010). Supplementary Methods. Nature, 463(7278), 1-14. doi: 10.1038/nature08705.